

Chapter

6

Basic physics of magnetism and NMR

Introduction	page 121
Electromagnetic fields	122
The field concept	122
Magnetic fields	123
Induction and NMR signal detection	125
Gradient and radiofrequency coils	128
Dynamics of nuclear magnetization	130
Interaction of a magnetic dipole with a magnetic field	130
Precession	131
Relaxation	131
Radiofrequency excitation	134
Frequency selective radiofrequency pulses: slice selection	136
Adiabatic radiofrequency pulses	139
Magnetic properties of matter	140
Paramagnetism, diamagnetism, and ferromagnetism	140
Magnetic susceptibility	142
Field distortions in the head	144

Introduction

In Ch. 3 the basic features of the NMR experiment were introduced, and in this chapter the basic physics underlying NMR is presented in more detail. We begin with a review of the basic physics of magnetic fields, including how coils are used to detect the NMR signal and how gradient fields are produced for imaging. The dynamics of a magnetic dipole in a magnetic field, which is the central physics underlying NMR, is considered next in terms of the two important physical processes of *precession* and *relaxation*. Precession and relaxation have quite different characteristics; precession is a rotation of the magnetization without changing its magnitude, whereas relaxation creates and destroys magnetization. The interplay of these two processes leads to a rich variety of dynamic behavior of the magnetization. In the final section of the chapter, the magnetic properties of matter are considered in terms of how the partial alignment of dipoles with the magnetic field creates additional fields in the body. These field variations caused by magnetic susceptibility differences between tissues lead to unwanted distortions in MR images, but such effects are also the basis for most of the fMRI techniques.

In trying to understand how NMR works, it is helpful to have an easily visualized model for the process. The physical picture presented here is a classical physics view, and yet the physics of a proton in a magnetic field is correctly described only by quantum mechanics. The source of the NMR phenomenon is that the proton possesses *spin*, and spin is intrinsically

a quantum mechanical property. Despite the familiar sounding name, spin is fundamentally different from the angular momentum of more familiar terrestrial scale objects. For example, a spinning baseball possesses angular momentum, and yet we can easily imagine changing that angular momentum by spinning it faster or stopping it altogether. In other words, the spin is not an intrinsic part of the baseball. But for a proton, the spin is an intrinsic part of being a proton. It never speeds up and never slows down, and the only aspect of the spin that can be changed is the orientation of the spin axis. Neutrons also possess spin, and protons and neutrons combine to form a nucleus such that their spins mutually cancel (opposite spin axes), so that the nucleus has no net spin unless there are an odd number of protons or neutrons. As a result, the nuclei of ^1H (one proton) and ^{13}C (six protons and seven neutrons) have a net spin, but ^{12}C does not.

Furthermore, the quantum view is still stranger, with only certain states allowed, and even the definition of a state is rather different from the classical view. At first glance, the quantum view seems to simplify the picture of the NMR phenomenon. The centerpiece of the quantum view is that any measurement of one component of the spin of a proton will yield only one of two possible values of the spin orientation: spin up or spin down. It seems as if this two-state system ought to be easier to think about than magnetic moment vectors that can point in any direction. However, this sort of partial introduction of quantum ideas into the description of NMR often leads to confusion. After all, if the spin can only be up or down in a magnetic field, how do we ever get transverse magnetization, precession, and the NMR signal? In short, the quantum view is correct, but it is difficult to think about the wide range of phenomena involved in NMR from a purely quantum viewpoint. Fortunately, however, the classical view, although totally incorrect in its description of the behavior of a single proton, nevertheless gives the correct physics for the *average* behavior of many protons, and accurately describes most of the physics encountered in MRI. For this reason, we will develop a physical picture of NMR based on a classical view, and the only feature from quantum mechanics that is essential is the existence of spin itself. For the interested reader, the Appendix contains a sketch of the quantum mechanical view of NMR.

Electromagnetic fields

The field concept

Nearly every aspect of the world around us is the result of the interactions of charged particles. Electrons in an atom are bound to the nucleus by the electric force between the charges, and light, and other forms of electromagnetic radiation, can be understood as the cooperative interplay among changing electric and magnetic fields. The phenomenon of NMR is, of course, deeply connected to magnetic field interactions, in particular the behavior of a magnetic dipole in a magnetic field. In addition, a recurring theme in MRI is the geometrical shape of the magnetic field, which underlies the design of coils for MRI, distortions in fast MRI, and the microscopic field variations that are the basis for the blood oxygenation level dependent (BOLD) signal changes measured during brain activation. To begin with, we consider the nature of magnetic fields. (Excellent introductions to electromagnetic fields are given by Purcell (1965) and Feynman *et al.* (1965).)

The concept of a field is a useful way of visualizing physical interactions, and the simplest example is a gravitational field. In comparison with the complex interactions of charged particles, the gravitational interaction of two massive bodies is relatively simple. The two bodies attract each other with a force that is proportional to the product of their masses and

inversely proportional to the square of the distance between them. We describe this interaction in terms of a field by saying that the second body interacts with the gravitational field created by the first body. The field extends through all of space, and the strength of the field at any point is proportional to the mass of the body and falls off with distance from the body with an inverse square law.

The gravitational field is a vector field in which each point in space has a vector arrow attached that describes the local strength and direction of the field. For visualizing a field, the most direct way is to imagine such arrows at every point in space, but this is difficult to draw. Instead, the usual way to show fields is to draw continuous *field lines*. A field line is an imagined line running through space such that the direction of the local field at any point on the line is tangent to the line. Each point in space has a field line running through it, but the field pattern can be graphically depicted by showing only selected field lines. Field lines naturally show the local field direction, but the magnitude of the local field is shown in a more subtle way. The stronger the field, the more closely spaced the field lines. Therefore, for the gravitational field around a spherical body, the field is drawn as radial lines pointed inward, with the spread of the field lines indicating the weakening of the field with increasing distance.

The electric field is in some ways analogous to the gravitational field, with electric charge playing the role of mass. The electric force between two charged bodies is proportional to the product of their charges and falls off with the square of the distance between them. However, there are two important differences between the electric field and the gravitational field: (1) the electric force between two like charges is repulsive, rather than attractive; and (2) charges can be either positive or negative, and the force between opposite charges is attractive. Because mass is always positive, gravity is always attractive and tends to pull matter into large massive bodies such as stars and planets. Because charges can be positive or negative, the electric force tends to group matter into smaller stable structures with no net charge, such as atoms and molecules.

The electric field can be represented graphically in the same way as the gravitational field, with the local vector arrows indicating the direction of the force on a positively charged particle (a negatively charged particle would feel a force in the opposite direction). For example, Fig. 6.1A shows the electric field around a positive charge, a *monopole field*. The field lines are radial and point outward, indicating that the force on another positive charge is repulsive. If the central charge were negative, the field lines would point inward like a gravitational field. However, because there are both positive and negative charges, there are electric field configurations that have no counterpart in a gravitational field. For example, Fig. 6.1B shows the field around two nearby charges with equal magnitude but opposite sign, a pattern known as an *electric dipole field*. There is no corresponding dipole gravitational field.

Magnetic fields

The existence of both positive and negative charges introduces some complexities into the interaction of charged particles, but the electric field is only a part of the picture. In addition to the electric interactions, there are additional forces generated by the motions of the charges. When a charged particle moves through a region where a magnetic field is present, the particle will feel a force in addition to that of any electric field that may be present. For example, consider two parallel wires carrying currents in the same direction. The positive and negative charges in each wire are balanced, so there is no electric force between the two wires. Yet experiments show that with parallel currents there is an attractive force between

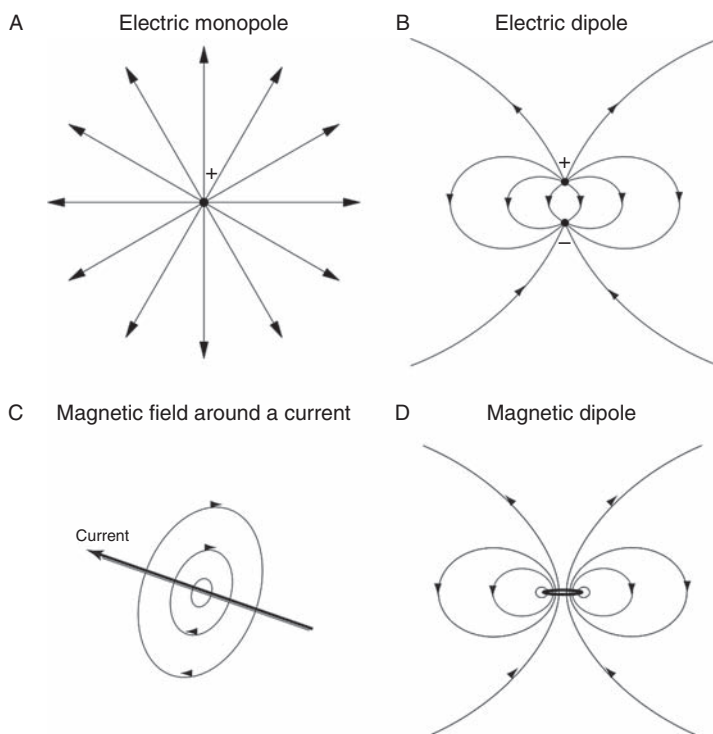


Fig. 6.1. Basic electric and magnetic field patterns. The simplest electric fields are the monopole field produced by a single charge (A) and the dipole field produced by two opposite and slightly displaced charges (B). There are no magnetic monopoles, and the simplest source of a magnetic field is a straight wire carrying a current (C). If the wire is bent into a small loop of current, the field is a magnetic dipole field (D). The electric and magnetic dipole fields are identical far from the source but are quite different near the source.

the two wires. If the current in one wire is reversed, the force becomes repulsive, and if the current in one wire is reduced to zero, the force disappears. This additional force is a result of the interaction of the moving charges in one wire interacting with the magnetic field created by the current in the other wire.

The force on a wire carrying a current in a magnetic field is the basis for a loudspeaker system, making possible the conversion of electrical signals into mechanical vibrations. It is also the source of the loud acoustic noise in an MR scanner. Imaging depends on applying pulsed gradient fields to the sample, which means that strong current pulses are applied to the gradient coils. These wires carry substantial current and are in a large magnetic field, so there are large forces produced, creating a sharp tapping sound when the gradients are pulsed. The sound can be quite loud, particularly when strong gradients are used, and subjects to be scanned must wear ear protection.

Magnetic fields are produced whenever there is a flow of electric charge creating a current. Figure 6.1C shows the magnetic field around a long straight wire. The field lines for this simple current are concentric circles in the plane perpendicular to the wire and centered on the wire. The direction of the field lines depends on the direction of the current, following a right-hand rule: with your right thumb pointing along the direction of the current, your fingers curl in the direction of the magnetic field. The magnetic field strength diminishes as the distance from the wire increases.

If a wire carrying a current is bent into a small circular loop, the magnetic field is distorted, as shown in Fig. 6.1D. Near the wire, the concentric field lines are similar to the straight wire. That is, if one is close enough to the current loop so that the curvature is not apparent, the magnetic field is similar to that of a straight wire. However, far from the source this

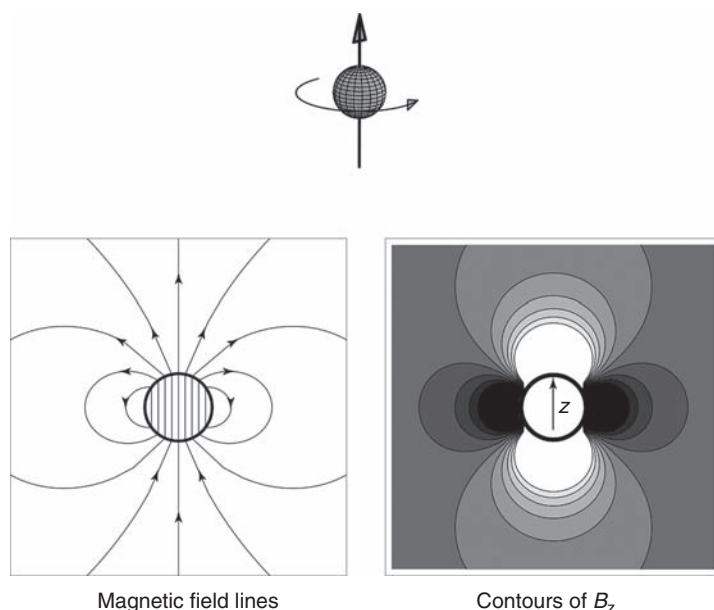


Fig. 6.2. The dipole field of a spinning charged sphere. A charged sphere rotating around the z -axis produces a magnetic dipole field outside. The field lines themselves are shown (B_z) but usually just the z -component of the field is of interest. Contours of equal B_z are shown on the right.

magnetic field pattern is identical to the electric dipole field, and, correspondingly, this pattern is called a *magnetic dipole field*. In general, the term *dipole field* refers to the pattern far from the source, and so two fields can be quite different near the source but still be described as dipole fields. For the electric dipole field, all the field lines end on one or the other of the two charges that make up the dipole. In contrast, the magnetic dipole field is composed of continuous loops that pass through the ring of current. This is a general and important difference in the geometry of electric and magnetic fields: magnetic field lines always form closed loops.

A small ring of current is the prototype of a magnetic dipole, but another classical example of a magnetic dipole is a spinning, charged sphere (Fig. 6.2). This is the basic picture of an atomic nucleus (e.g., the proton, the nucleus of hydrogen) often used for visualizing NMR. For simplicity, assume that the charge is uniformly distributed over the surface of the sphere. This rotating sphere can be viewed as a stack of current loops, with the largest loop area and highest current at the equator of the sphere. When these loops are summed, the net magnetic dipole moment of the sphere turns out to be identical to that of a single current loop at the center of the sphere. Figure 6.2 illustrates the magnetic dipole field by plotting both the field lines and a contour map of just the z -component of the magnetic field (B_z). (For most NMR applications, the z -component of additional fields are important because this is what adds to the main magnetic field [B_0] to create field variations.)

Induction and NMR signal detection

Our picture of electromagnetic fields so far is that charges create electric fields, and charges in motion (currents) create magnetic fields. In the first half of the nineteenth century, Faraday unraveled an additional feature: *changing* magnetic fields create electric fields. This phenomenon, called *electromagnetic induction*, is at the heart of many examples of electrical technology. For example, induction makes possible the generation of electricity from a mechanical

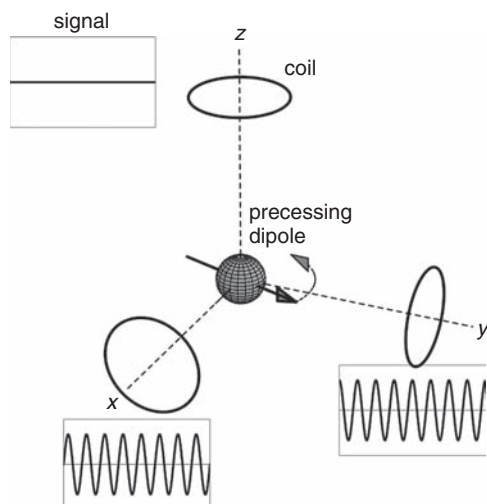


Fig. 6.3. Induction signals in coils near a precessing magnetic dipole. For a dipole rotating in the x - y plane, coils along the x - and y -axis show oscillating signals with a relative phase shift of 90° as the magnetic flux of the dipole sweeps across the coils. For the coil along the z -axis, the flux is constant, and so no current is induced.

energy source, such as hydroelectric power, and the conversion of acoustic signals into electrical signals in a microphone.

In NMR, induction is the process that generates a measurable signal in a detector coil. Imagine a small dipole moment, a spinning charged sphere, rotating around an axis perpendicular to its spin axis. The spinning sphere creates a dipole magnetic field in its vicinity, and as the magnet rotates the dipole field sweeps around as well. As a result, at any fixed point in space near the magnetic dipole, the magnetic field changes cyclically with time. If we now place a loop of wire, a detector coil, near the spinning dipole, the changing magnetic field will create a current in the wire through the process of induction (Fig. 6.3).

The strength of the induced current in the coil depends on both the proximity and the orientation of the coil with respect to the magnetic dipole. The quantitative relation is that the induced current is proportional to the rate of change of the *flux* of the magnetic field through the coil. For example, consider a circular coil and imagine the surface enclosed by the wire. The net flux of the magnetic field is calculated by adding up the perpendicular components of the magnetic field lines at each point on this surface. Or, more qualitatively, the flux is proportional to the number of field lines enclosed by the coil.

The somewhat abstract concept of magnetic flux suggests a flow of something through the coil, but the thing “flowing” is the magnetic field. The source of the terminology is a close analogy between magnetic fields and velocity fields in a fluid. Velocity is also a vector, and the velocity field within a fluid can be plotted as a field with the same conventions that we use for the magnetic field. Velocity field lines in an incompressible fluid also form closed loops, like magnetic field lines. Placing our coil in the fluid, the calculated flux is simply the volume flow rate through the coil. When the coil is perpendicular to the local flow direction, the flux is high; if the coil is placed so that the flow passes over it rather than through it, the flux is zero.

Figure 6.3 illustrates a spinning magnetic dipole inducing currents in several nearby coils. Note that when the coil is oriented such that the axis of the coil is the same as the axis of rotation of the dipole, the flux is constant so there is no induced current. For other orientations though, a cyclic signal is generated in the coil with the same frequency as the

frequency of rotation of the dipole. The maximum signal is produced when the axis of the coil is perpendicular to the axis of rotation of the dipole, because this orientation creates the largest change in flux as the dipole field sweeps past the coil. When the coil is moved farther from the source, the flux is diminished, and so the change in flux also is diminished, and the signal created in the coil is weaker.

The two coils oriented 90° from each other, but with the axis of each coil perpendicular to the rotation axis, show the same strength of induced current, but the signals are shifted in time. This time shift of the signal is described as a *phase shift*, and in this case it is a phase shift of 90° . For any periodic signal with a period T , a shift in time can be described as an angular phase shift in analogy with circular motion. A phase shift of one full period T corresponds to one complete cycle, while a phase shift of 360° , and a time shift of $T/4$ corresponds to a phase shift of 90° . Sometimes phase shifts are expressed in radians rather than degrees, where $360^\circ = 2\pi$ radians.

The concept of phase recurs often in MRI. In particular, the concept of *phase dispersion* and a resulting loss in signal is important in virtually all MRI techniques. Imagine a coil detecting the signal from several rotating dipoles. If the dipoles are all rotating in phase with one another, so that at any instant they are all pointing in the same direction, then the signals induced by each in the coil add coherently and create a strong net signal. However, if there is phase dispersion, so that at any instant the dipoles are not aligned, then there is destructive interference when the signals from each dipole are added together in the coil, and the net signal is reduced.

The configuration of two coils perpendicular to each other is an example of a *quadrature detector*. Each coil is sensitive to the component of the magnetization perpendicular to the coil because that is the component that creates a changing flux through the coil. Because of their orientation, the signal measured in the second coil is phase-shifted 90° from the signal in the first coil. By electronically delaying the second signal for one quarter of a cycle, the two signals are brought back in phase and can be averaged to improve the signal to noise ratio (SNR) before being sent to the amplifier. Noise comes about primarily from fluctuating stray currents in the sample, which create random currents in the detector coil. Because the two coils of a quadrature detector are oriented perpendicular to each other, the fluctuating fields that cause noise in one coil have no effect on the other coil. If the fluctuating fields along these two directions are statistically independent, the noise signals measured in the two coils will also be independent. Then when the signals from the two coils are combined, the incoherent averaging of the noise improves the SNR by $\sqrt{2}$ compared with a single-coil measurement.

In a *phased array* coil arrangement, two or more coils send signals to separate amplifiers, with the result that the detected signals are analyzed individually. Phased array coils are useful for imaging as a way of improving the SNR beyond what can be achieved by quadrature detection alone (Grant *et al.* 1998). The noise picked up by a coil is proportional to its sensitive volume, which is linked to the size of the coil. Therefore, a small coil has a higher SNR, but the drawback of a small coil is that only a small region can be imaged. With a phased array system, several small coils can be used to achieve the coverage of a large coil but with the SNR of a small coil. Each coil is sensitive to a different location and so provides a high SNR for the signal from that location. Note that this requires separate amplifier channels for each coil. If the signals from the different coils were combined before being sent to a single amplifier, the noise from each coil would contaminate the signals from the other coils, destroying the SNR advantage.

Gradient and radiofrequency coils

Any configuration of wires carrying a current creates a magnetic field in the vicinity of the wires. We will refer to any such arrangement as a coil, even if it is not a simple loop or helical configuration. In MRI, coils are used for generating the main magnetic field for generating gradient fields used for imaging, for generating the oscillating radiofrequency (RF) field used to tip over the local magnetization, and for detecting the NMR signal. A surface coil for detecting the signal may be as simple as a single loop of wire, but the designs of more complex RF and gradient coils are much more sophisticated. Nevertheless, we can appreciate how different field patterns can be created by considering two prototype coil configurations produced by combining two circular coils carrying a current. The field of each coil separately was shown in Fig. 6.1, and the net fields for two coil arrangements are illustrated in Fig. 6.4. Each set consists of two circular coils oriented on a common axis, with the currents parallel in the first set (Fig. 6.4A) and opposite in the second set (Fig. 6.4B).

The first arrangement, called a Maxwell pair, produces a rather uniform field between the two coils, with the field diverging and weakening at the two ends. If many such coils are stacked together, the result is a solenoid with a very uniform field inside. This is the basic coil

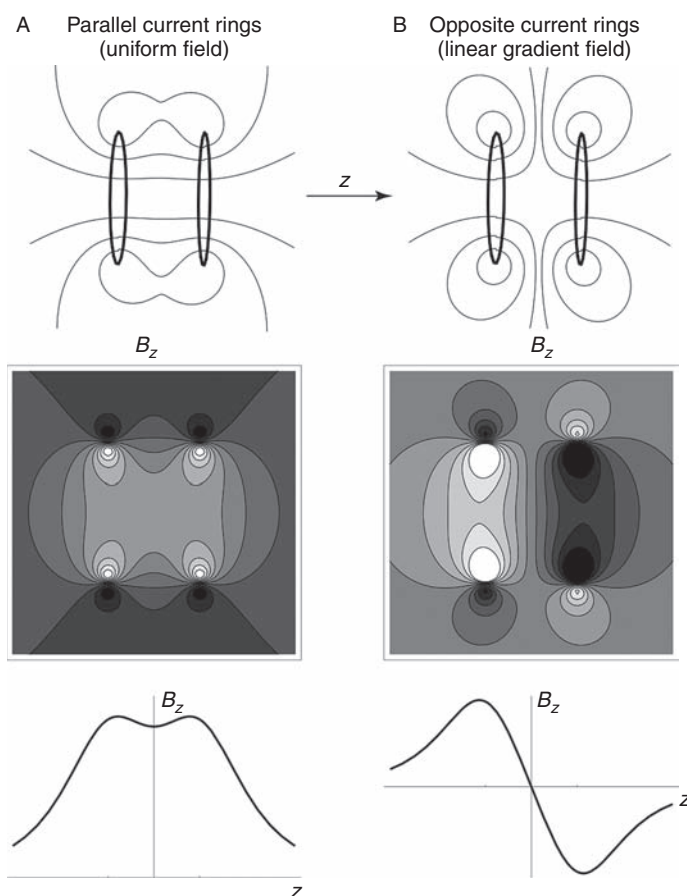


Fig. 6.4. Two simple coil configurations suggest how the geometry of magnetic fields can be manipulated. (A) Two circular coils with parallel currents, called a Maxwell pair, create a roughly uniform field between them, a prototype for the solenoid current arrangement that generates a uniform main magnetic field B_0 . (B) Two circular coils with opposite currents, called a Helmholtz pair, generate a linear gradient field in the region between them, a prototype for the gradient coils used for imaging. The top row shows the field lines, the middle row shows contour plots of the z -component of the magnetic field (B_z), and the bottom row shows plots of B_z versus z along the axis of the coils.

design used for creating B_0 in an MRI system, and in a commercial scanner the field variation over a central region of approximately 20 cm is less than a few tenths of a part per million. The field strength depends on the total current flowing through the coil, and large, uniform magnetic fields can be created when superconducting (zero resistance) coils are used.

The arrangement of two coils with currents running in opposite directions is known as a Helmholtz pair. The effect of this arrangement is that the fields created by the two loops tend to cancel in the region halfway between them. Moving off-center along the coil axis, the field increases in one direction and decreases in the other direction. This type of field is called a *gradient field*, and gradient fields are a critical part of MRI. In an MR imager, the gradient coils produce additional fields, which add to B_0 . The direction of B_0 is usually defined as the z -axis, and the goal with a gradient coil is to produce an additional field along z such that B_z varies linearly along one axis. In practice, the designs for linear imaging gradients are more sophisticated than this simple Helmholtz pair to improve the linearity and homogeneity of the field. That is, for an ideal linear gradient coil the field component B_z varies linearly moving along the coil axis but is uniform moving perpendicular to the coil axis.

In imaging applications, we are interested in just the z -component of the field offset because that is the only component that will make a significant change in the net field amplitude and so affect the resonant frequency. A weak field component, of the order of a few parts per million, perpendicular to B_0 will produce a change in the total field magnitude of the order of 10^{-12} , a negligible amount. But an offset in B_z itself of a few parts per million will directly alter the total field strength, and thus the resonant frequency, by a few parts per million. Offsets of this magnitude are comparable to the field offsets between one voxel and its neighbor during frequency encoding in MRI. The important effect of gradient fields for imaging is that they modify the z -component, producing a gradient of B_z .

The preceding discussion suggests how different coil configurations can be used to generate different patterns of magnetic field. However, when a coil is used for signal *detection*, the physics at first glance seems to be rather different. As described in the previous section of this chapter, the current induced in a coil by a local precessing magnetization is proportional to the changing magnetic flux through the coil. Fortunately, it turns out that there is a simple relation between the magnetic field *produced* by a coil when a current is run through it and the current *induced* in the coil by an external changing magnetic field. For any coil used as a detector, an associated *sensitivity* pattern describes the strength of the signal produced in the coil by sources at different locations in space. One could calculate the sensitivity map by placing rotating dipoles at many positions relative to the coil and using the changing magnetic flux rule to determine the induced current. However, this sensitivity pattern also can be calculated from a useful rule called the *principle of reciprocity*: the sensitivity of any coil to a rotating magnetic dipole at any point in space is directly proportional to the magnetic field that would be produced at that point in space by running a current through the coil. Specifically, imagine a precessing magnetic dipole M sitting near a coil, and consider the magnetic field vector \mathbf{b} that would be produced at the location of the dipole by running a unit current through the coil. The signal produced in the coil by the dipole depends directly on the vector \mathbf{b} : the signal is proportional to the product of the magnitude of \mathbf{b} and the component of M that lies along \mathbf{b} (i.e., the scalar product of \mathbf{b} and M). For example, if the arrangement of the coil is such that \mathbf{b} is perpendicular to M (such as a circular coil with its axis along z), no signal is generated. For any orientation, the magnitude of \mathbf{b} is small far from the coil, so the sensitivity of the coil is weak. Therefore, an RF coil can be thought of

as having two roles: a producer of magnetic fields and a detector of changing magnetic fields. The geometrical pattern associated with each is the same.

Dynamics of nuclear magnetization

Interaction of a magnetic dipole with a magnetic field

In the previous discussion, we focused on the magnetic field created by a magnetic dipole. In NMR, the fundamental interaction is between the magnetic dipole moment of the atomic nucleus and the local external magnetic field, which is characterized by two basic effects. The first is that the field exerts a torque on the dipole that tends to twist it into alignment with the field, and the second is that in a non-uniform field there is a force on the dipole pulling it toward the region of stronger field. These effects are most easily understood by considering an electric dipole in an electric field. A magnetic dipole in a magnetic field behaves in the same way as the electric dipole, but the physical arguments that demonstrate this are more subtle (details are given in the Appendix).

An electric dipole can be thought of as two opposite charges attached to a rod of fixed length, with the direction of the dipole vector running from the negative to the positive charge. When the dipole is placed at an angle to a uniform electric field (Fig. 6.5), there is a moment arm between the points where the two forces are applied, and the result is a torque on the dipole. One end is pulled up, the other is pushed down, and the dipole pivots around the center. The only stable configuration for the dipole is when it is aligned with the field. When the dipole is placed in a non-uniform electric field, again the field will produce a torque that will align the dipole with the field. However, because the field is not uniform, the forces on the positive and negative charges do not balance even when the dipole is aligned with the field; the force down on the lower charge is stronger than the force up on the positive charge in Fig. 6.5. The result is that there is a net force downward on the dipole, pulling the dipole toward the region of stronger field. If the dipole is aligned opposite to the field, the force also is opposite, pushing the dipole toward the region of weaker field. However, such an alignment would be unstable for an electric dipole: the torque would twist it 180°, and it would be pulled toward the region with a stronger field.

Both of these effects can be described in an equivalent way in terms of the energy of a dipole in a field. The dipole has the lowest energy when it is aligned with the field, and the energy progressively increases as the dipole is tipped away from the field. The highest energy configuration is when the dipole is aligned opposite to the field. Similarly, the energy of the

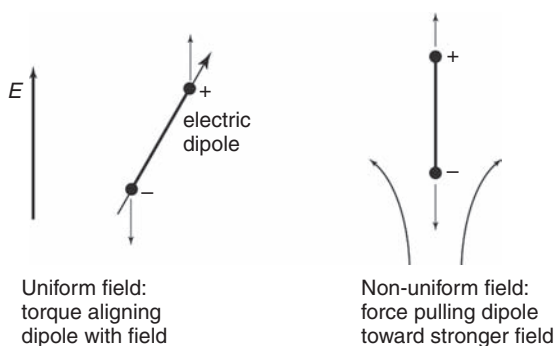


Fig. 6.5. Dipole interactions with a field. The nature of the forces is most easily illustrated by an electric dipole placed in an electric field E . An electric dipole consists of two opposite charges separated by a short distance, and an external field exerts a torque acting to align the dipole with the field and a force drawing the aligned dipole into regions of stronger field. (Forces are shown as thin arrows.)

dipole is lower when it is in a stronger field, so it is drawn toward regions with a larger field. Both alignment with the field and moving toward stronger fields are then examples of the system seeking a lower energy state.

Precession

A magnetic dipole placed in a magnetic field experiences the same two effects: a torque tending to align the dipole with the field and a force drawing it toward regions of stronger field. However, for a nuclear magnetic dipole the intrinsic angular momentum of the nucleus changes the dynamics in a critical way. Viewing a magnetic dipole as a rotating charged sphere brings out the close connection between the magnetic moment and the angular momentum. Both the angular momentum and the magnetic dipole moment are proportional to the rate of spin of the sphere. Faster rotation increases the angular momentum as well as the current produced by the charges on the surface, and so also increases the magnetic moment. Because of this intimate link between angular momentum and the magnetic dipole moment, the ratio of the two is a constant called the *gyromagnetic ratio* (γ). Each nucleus that exhibits NMR has a unique value of γ .

The presence of angular momentum makes the dynamics of a magnetic dipole in a magnetic field distinctly different from the dynamics of an electric dipole in an electric field. As already described, the effect of the field is to exert on the dipole a torque that would tend to twist it into alignment. Physically, torque is the rate of change of angular momentum, analogous to Newton's first law that force is the rate of change of momentum. Precession comes about because the torque axis is perpendicular to the existing angular momentum around the spin axis. The *change* in angular momentum then is along the direction of the torque and so is always perpendicular to the existing angular momentum. In other words, the change in angular momentum produced by the torque is a change in the *direction* of spin, not the magnitude. Thus, the angular momentum (and the spin axis) precesses around the field. (A more mathematical derivation of precession is given in the Appendix.)

This is an example of the peculiar nature of angular momentum and is exactly analogous to the behavior of a spinning top or bicycle wheel. A spinning top tipped at an angle to the vertical would be in a lower energy state if it simply fell over; instead, the rotation axis precesses around a vertical line. For a nucleus in a magnetic field, the frequency of precession, called the *Larmor frequency* (ω_0), is γB_0 ; the stronger the field, the stronger the torque on the dipole and the faster the precession. We will use the convention that when frequency is represented by ω , it is expressed as angular frequency (radians per second), and when it is represented by ν , it is expressed as cycles per second (Hz), with the relation $\omega = 2\pi \nu$. The equation for the Larmor frequency holds regardless of whether we are using angular frequency or cycles per second, with a suitable adjustment in the magnitude of γ . The precession frequency $\omega_0 = \gamma B_0$ is the resonant frequency of NMR.

Relaxation

The foregoing considerations apply to a single nucleus in a magnetic field. From the precession arguments alone, one might conclude that a proton would never align with the main field, despite the fact that the energy is lower. However, in a real sample, B_0 is not the only source of magnetic field. The magnetic moments of other nuclei produce additional, fluctuating magnetic fields. For example, in a water molecule, an H nucleus feels the field produced by the other H nuclei in the molecule. Because the molecules are rapidly tumbling in their thermal motions, the total field felt by a particular nucleus fluctuates around the mean field B_0 . These

fluctuations alter both the magnitude of the total magnetic field and the direction felt by that nucleus. As a result, the proton's precession is more irregular, and the axis of precession fluctuates. Over time, the protons gradually tend to align more with B_0 , through the process called *relaxation*. Note, though, that relaxation is a much slower process than precession: relaxation times on the order of 1 s are approximately 10^8 times longer than the precession period with a typical MRI magnet.

Because the energy associated with the orientation of the magnetic dipole moment of an H nucleus in a magnetic field is small compared with the thermal energy of a water molecule, the average degree of alignment with the field is small, corresponding to a difference of only approximately 1 part in 10^5 between those nuclei aligned with the field and those opposite. However, this is sufficient to produce a slight net equilibrium magnetization (M_0) of the water. The creation of M_0 can be understood as a relaxation toward thermal equilibrium. When a sample is first placed in a magnetic field, the magnetic dipoles are randomly oriented so that the net magnetization is zero. This means that the dipoles possess a higher energy based on their orientation than they would if they were partly aligned with the field. (The lowest possible energy would correspond to complete alignment.) As the system relaxes, this excess energy is dissipated as heat; the dipoles align more with the field, and the longitudinal magnetization M grows toward its equilibrium value M_0 .

In a pure water sample, the main source of a fluctuating magnetic field that produces relaxation is the field produced by the other H nucleus in the same water molecule. But the presence of other molecules in the liquid (e.g., protein) can alter the relaxation rate by changing either the magnitude or the frequency of the fluctuating fields. A large molecule will tumble more slowly than a water molecule and, as a result, a water molecule that transiently binds to the large molecule will experience more slowly fluctuating fields. The magnitude of the fluctuating fields can be increased significantly in the presence of paramagnetic compounds. Paramagnetic compounds have unpaired electrons, and electrons have magnetic moments more than a thousand times larger than a proton. This is the basis for the use of paramagnetic contrast agents, such as gadolinium-labeled diethylenetriaminepentaacetic acid (Gd-DTPA), as a way of reducing the local relaxation time. The physical sources of the relaxation times are discussed more fully in Ch. 7.

The time constant for relaxation along the magnetic field, creating the net magnetization M_0 , is T_1 and varies from approximately 0.2 to 4.0 s in the body. The fact that T_1 varies by an order of magnitude between different tissues is important because this is the source of most of the contrast differences between tissues in MR images. The T_1 variations result from differences in the local environment (e.g., chemical composition or biological structures). In general, the higher the water content of a tissue, the longer the T_1 . The strong dependence of the relaxation time on the local environment is exactly analogous to everyday experiences of relaxation phenomena. A cup of hot coffee sitting in a cool room is not in thermal equilibrium. Over time, the coffee will cool to room temperature (thermal equilibrium), but the time constant for this relaxation depends strongly on the local environment. If the coffee is in a thin-walled open cup, it may cool in a few minutes, whereas if it is in a covered, insulated vessel, it may take hours to cool. Regardless of how long it takes to get there, the final equilibrium state (cold coffee) is the same. Similarly with NMR relaxation, the value of M_0 depends on the density of dipoles and the magnetic field, but the value of T_1 required to reach this equilibrium depends on the environment of the spins.

The relaxation time T_1 is called the *longitudinal* relaxation time because it describes the relaxation of the component of the magnetization that lies along the direction of B_0 . Two

other relaxation times, T_2 and T_2^* , describe the decay of the *transverse* component of the magnetization. At equilibrium, the magnetization is aligned with B_0 , so there is no transverse component. Application of a 90° RF pulse tips the magnetization into the transverse plane, where it precesses and generates a signal in a detector coil by induction. In a homogeneous field, the transverse component, and therefore also the NMR signal, decays away with a time constant T_2 , and this process often is abbreviated as transverse relaxation. In the human body at field strengths typical of MR imagers, T_1 is approximately 8–10 times larger than T_2 .

In practice, one finds experimentally that the NMR signal often decays more quickly than would be expected for the T_2 of the sample. This is qualitatively described by saying that the decay time is T_2^* , with T_2^* less than T_2 . The reason for this is simply inhomogeneity of the magnetic field. If two regions of the sample feel different magnetic fields, the precession rates will differ, the local transverse magnetization vectors will quickly get out of phase with each other, and the net magnetization will decrease through phase dispersion. However, this signal decay results from constant field offsets within the sample and not the fluctuating fields that produce T_2 decay. Because of this, the additional decay caused by inhomogeneity is reversible with a spin echo, introduced in Ch. 3 and discussed in more detail in Ch. 7.

The combined processes of precession and relaxation are mathematically described by the *Bloch equations*, a set of differential equations for the three components of the magnetization (Box 6.1). These are the basic dynamic equations of NMR and are used frequently to describe the behavior of the magnetization.

Box 6.1. The Bloch equations

Early in the development of NMR, Bloch proposed a set of differential equations to model the dynamics of the magnetization produced by nuclear magnetic dipoles in a magnetic field. The equations include precession, as derived above, and also exponential relaxation with relaxation times T_1 and T_2 . The representation of relaxation is essentially empirical, designed to reproduce the experimentally observed exponential dynamics. The Bloch equations are still the basic equations used to understand the magnitude of the NMR signal. The equations are written separately for the three components of the magnetization, M_x , M_y , and M_z in a magnetic field B_0 along the z -axis:

$$\frac{dM_x}{dt} = \gamma B_0 M_y - \frac{M_x}{T_2}$$

$$\frac{dM_y}{dt} = -\gamma B_0 M_x - \frac{M_y}{T_2}$$

$$\frac{dM_z}{dt} = -\frac{M_z - M_0}{T_1}$$

Precession is incorporated into the equations in the way that the rates of change of the two transverse components, M_x and M_y , depend on the current values because precession rotates M_x partly into M_y , and vice versa. Relaxation is described by a steady decrease of the transverse component by the transverse relaxation rate, $1/T_2$, and relaxation with a rate $1/T_1$ of the M_z component toward the equilibrium magnetization M_0 . If we start with an arbitrary magnetization

vector, with a transverse component $M_{xy}(0)$ and a longitudinal component $M_z(0)$, the magnitudes of these components at later times given by the solution of the Bloch equations are:

$$M_{xy} = M_{xy}(0) e^{-t/T_2}$$

$$M_z = M_0 - [M_0 - M_z(0)] e^{-t/T_1}$$

In addition to these magnitude changes, the full solution also includes precession of the transverse component with frequency γB_0 .

The transverse component decays exponentially with time constant T_2 . The relaxation of the longitudinal component can be described as an exponential decay with time constant T_1 of the difference between the starting value $M_z(0)$ and the equilibrium value M_0 . In fact, we could describe both decay processes as an exponential decay of the *difference* between the initial state and the equilibrium state, and the equilibrium state is M_0 along M_z and a transverse component of zero.

The preceding equations describe relaxation and free precession when the only magnetic field acting on the magnetization is B_0 . To describe what happens during the RF pulse, we must also include the effects of an oscillating field B_1 . This is most easily represented in a frame of reference rotating at the frequency of B_1 oscillations, ω . This transformation essentially takes out the basic precession and simplifies the equations. In this rotating frame, B_1 appears to be constant, and we can take it to lie along the x -axis. Also, the apparent precession rate of M caused by B_0 in this rotating frame is reduced to $\omega_{\text{rot}} = \omega_0 - \omega$, and so it appears as if the magnetic field in the z -direction has been reduced to $B_z = B_0 - \omega_1/\gamma$. The effective magnetic field (B_{eff}) in the rotating frame then has two components, B_1 along the x -axis and B_z along the z -axis, and the dynamics of M is then precession around B_{eff} plus relaxation. If we represent the amplitude of B_1 as an equivalent precession frequency $\omega_1 = \gamma B_1$ (the rate at which M would precess around B_1), the Bloch equations in the rotating frame take the form:

$$\frac{dM_x}{dt} = \omega_{\text{rot}} M_y - \frac{M_x}{T_2}$$

$$\frac{dM_y}{dt} = -\omega_{\text{rot}} M_x - \frac{M_y}{T_2} + \omega_1 M_z$$

$$\frac{dM_z}{dt} = -\frac{M_z - M_0}{T_1} - \omega_1 M_y$$

This form of the equations clearly shows how the dynamics of the magnetization depends on four distinct rate constants: the off-resonance frequency of B_1 , ω_{rot} ; the amplitude of B_1 expressed as a precession frequency, ω_1 ; and the two relaxation rates, $1/T_2$, and $1/T_1$. Different proportions of these parameters produce a wide range of dynamics. Furthermore, in a tailored RF pulse, the amplitude of B_1 is a function of time, and in an adiabatic pulse the off-resonance frequency is also a function of time.

Radiofrequency excitation

Nuclear magnetic resonance is a transient phenomenon. The fact that the magnetic dipole moments of protons tend to align with the field, producing a net magnetization M_0 , does not lead to any measurable signal (a constant magnetic field produces no currents). However, if

M_0 is tipped away from the direction of B_0 , it will precess; all the nuclear dipoles will precess together if they are tipped over, so M_0 also will precess at the same frequency. The transverse component of M_0 then produces a changing magnetic field and will generate a transient NMR signal in a nearby detector coil by induction.

The tipping of the magnetization is accomplished by the RF pulse, an oscillating magnetic field B_1 perpendicular to B_0 and oscillating at the proton precession frequency. It is simplest to picture B_1 as a small magnetic field with constant amplitude in the transverse plane that rotates at a rate matched to the proton precession rate. Such a field is described as a *circularly polarized* oscillating field. When B_1 is turned on, the net field, the vector sum of B_0 and B_1 , is tipped slightly away from the z -axis and rotates over time. Because M_0 along the z -axis is no longer aligned with the net magnetic field, it begins to precess around the net field even as that field itself rotates. In other words, the basic physical process involved with the RF pulse is still just precession of M_0 around a magnetic field, but it is now more difficult to picture because the magnetic field itself is also rotating as the magnetization tries to precess around it. To understand the complexity of this process, a useful conceptual tool is the *rotating frame of reference*.

To introduce the rotating frame, forget B_1 for the moment and picture a magnetization vector M tipped away from the z -axis (Fig. 6.6). We know that in the laboratory frame of reference, the magnetization will simply precess around the field B_0 lying along the z -axis. We will ignore relaxation effects for now as well and assume that we are watching the magnetization for a short enough time that relaxation effects are negligible. Because the time scale for precession is so much shorter than that for relaxation, we could observe the precession for thousands of cycles with no detectable effects from relaxation. Now imagine that we observe this precession from a frame of reference that is itself rotating at the Larmor frequency ($\omega_0 = \gamma B_0$). In this frame, we are carried around at the same rate as the precession, as though we were riding on a turntable, and so in the rotating frame the magnetization appears to be stationary. Because there appears to be no precession in the rotating frame, it appears as if there is no magnetic field (i.e., as if B_0 is zero). Now suppose that we are in a rotating frame rotating with an arbitrary angular frequency ω . In this new rotating frame, the magnetization precesses around the z -axis, but with an effective angular frequency $\omega_0 - \omega$.

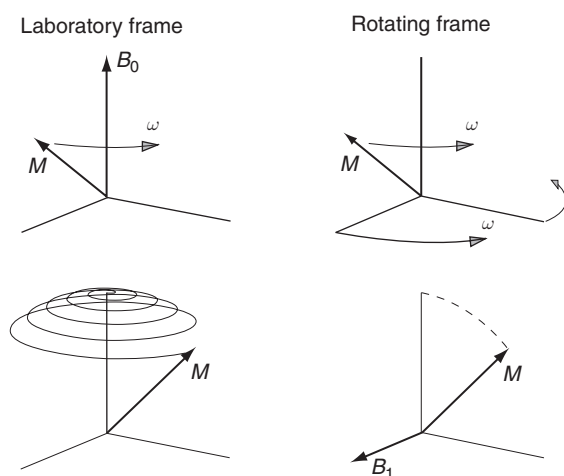


Fig. 6.6. The rotating frame of reference. In the laboratory frame of reference, the magnetization (M) precesses around the magnetic field (B_0) with a frequency ω . In a frame of reference rotating at the same rate, the magnetization appears to be stationary, so in this frame there appears to be no magnetic field. A radiofrequency (RF) field B_1 rotating at the resonant frequency appears stationary in the rotating frame, and RF excitation is then a simple precession of M around B_1 in the rotating frame. In the laboratory frame, this motion is a slowly widening spiral.

In other words, the magnetization behaves in this rotating frame exactly as it would in a stationary frame if the magnetic field were reduced from B_0 to $B_0 - \omega/\gamma$. This is the power of the rotating frame as a conceptual tool: the physics of precession is the same in a rotating frame as in a stationary frame, but the apparent magnetic field in the rotating frame is changed.

We can now return to the RF pulse and look at B_1 in the frame rotating with angular velocity ω , the oscillation frequency of B_1 . To begin with, we will assume that B_1 is oscillating on-resonance with the protons ($\omega = \omega_0$), and we will return to consider off-resonance effects later. In the rotating frame, B_1 is constant, and we will call its direction the x -axis of the rotating frame. When B_1 is on-resonance, the apparent field along the z -axis is zero in the rotating frame. This means that from this perspective there is only the field B_1 along x , so M_0 begins to precess around the x -axis in the rotating frame. The RF field B_1 is much weaker than B_0 , so the rate of precession around B_1 is correspondingly slower. But if we wait long enough (perhaps a few milliseconds for the RF pulses used in imaging), the magnetization will rotate around B_1 , tipping away from the z -axis and toward the y -axis of the rotating frame. If B_1 is left on long enough to tip M_0 fully on to the y -axis, the RF pulse is called a 90° pulse. If left on longer, or if the amplitude of B_1 is increased, the flip angle can be increased to 180° or even 360° , which would leave M_0 where it started along the z -axis. Thus, the complex picture of precession around a time-varying magnetic field in the laboratory frame is reduced to a simple precession around B_1 in the rotating frame. To picture the full dynamics of the magnetization as it would appear in the laboratory frame, this slow precession around B_1 must be added to a rapid precession of the rotating frame itself around the z -axis. The net result in the laboratory frame is a tight spiral that slowly increases the angle between M_0 and B_0 (Fig. 6.6).

After B_1 is turned off, M_0 continues to precess around B_0 and generates a signal in the detector coil. The signal is called a *free induction decay* (FID), where *free* relates to free precession, *induction* is the physical process described above in which a varying magnetic field (the precessing magnetization) produces a current in a coil, and *decay* indicates that the signal eventually dies out. Over time, M_0 will relax until it is again aligned with B_0 . Because the action of an RF pulse is to tip M_0 away from B_0 , such pulses usually are described by the *flip angle* (or *tip angle*) they produce (e.g., a 90° RF pulse or a 180° RF pulse). The flip angle is adjusted by changing either the duration or the amplitude of B_1 .

From the thermodynamic point of view, the process of tipping M_0 can be interpreted as the system of magnetic dipoles absorbing energy from the RF field because the alignment of M_0 is changing and then dissipating this energy over time as heat as the system relaxes back to equilibrium. For this reason, the RF pulse is often described as an *excitation pulse* because it raises the system to an excited (higher energy) state.

Frequency selective radiofrequency pulses: slice selection

In the previous description of the RF pulse, we assumed that B_1 was oscillating at precisely the resonant frequency of the protons, ω_0 . What happens if the RF pulse is off-resonance? This is an important question for imaging applications because the process of *slice selection*, which limits the effects of the excitation pulse to just a thin slice through the body, is based on the idea that an RF pulse far off-resonance should have a negligible effect on the magnetization. Slice selection is accomplished by turning on a magnetic field gradient during the RF pulse so that the resonant frequency of spins above the desired slice will be higher, and that of spins below the slice will be lower, than the frequency of the RF pulse. The RF pulse

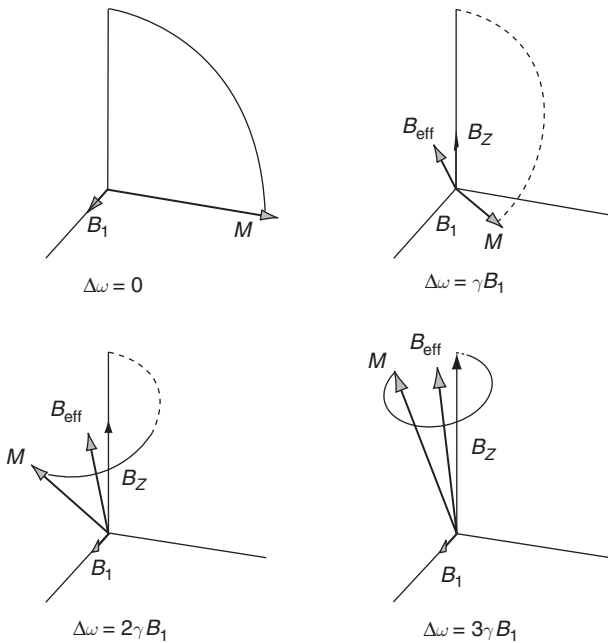


Fig. 6.7. Off-resonance excitation. The effect of an off-resonance radiofrequency (RF) pulse (B_1) can be understood as precession around the effective field in the rotating frame. Because the rotation of the frame differs from the precession frequency of the magnetization (M), the precession of M in the rotating frame is equivalent to precession in a magnetic field B_z . The vector sum of B_1 and B_z is the effective field B_{eff} . When B_1 is on-resonance (top left), the effect is a simple 90° flip of M , but as the off-resonance frequency $\Delta\omega$ is increased, the RF pulse is less effective in tipping over M .

will then be on-resonance for the spins at the center of the slice, and only these will be tipped over. However, for spins slightly removed from the central slice plane, the RF pulse will only be a little off-resonance, so we would expect that these spins will be partly flipped, but not as much as those at the center. The slice profile, the response of spins through the thickness of the slice, will then depend on the degree of tipping produced by a slightly off-resonance RF pulse. The most desirable slice profile is a perfect rectangle because this means that the slice has a well-defined slice thickness and a sharp edge. In practice, this cannot be achieved, but with carefully tailored RF pulses the slice profile approaches a rectangle.

We can understand the physics of off-resonance excitation by returning to the frame of reference rotating at the oscillation frequency ω of B_1 , and we will now relax our earlier assumption that ω is equal to ω_0 (Fig. 6.7). If ω and ω_0 are different, then in the rotating frame the magnetization behaves as though there were an apparent field along the z -axis of $B_z = B_0 - \omega/\gamma$. In other words, in the absence of B_1 , the magnetization would precess in the rotating frame around the z -axis with an angular frequency $\omega_0 - \omega$. When B_1 is turned on along the x -axis in the rotating frame, the effective field B_{eff} is the vector sum of B_z and B_1 , and so is a vector lying somewhere in the x - z plane. If B_1 is nearly on-resonance, then $\omega_0 - \omega$ is small and B_z is small, so B_{eff} points only slightly away from the x -axis. But if the frequency of B_1 is far off-resonance, B_{eff} points nearly along the z -axis. The effective field is constant in the rotating frame, so the motion of M_0 is simply a precession around B_{eff} with angular frequency γB_{eff} for the duration of the B_1 pulse.

Qualitatively, then, we can see why a far off-resonance pulse does little tipping of the magnetization because, with B_{eff} nearly aligned with the z -axis, the precession around B_{eff} leaves M_0 very near to its original orientation along the z -axis (Fig. 6.7). More quantitatively, this picture can be used to calculate the effects of off-resonance excitation, and thus the slice

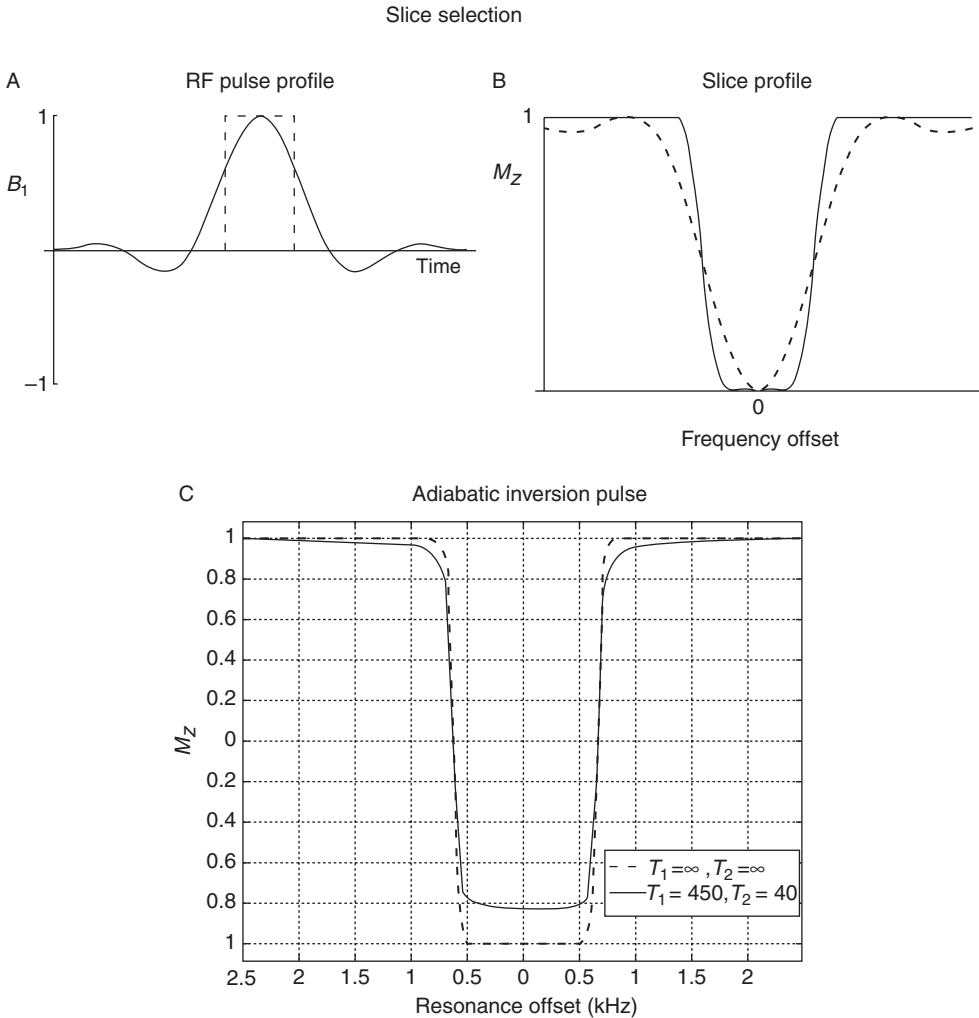


Fig. 6.8. Slice selection with frequency-selective radiofrequency (RF) pulses. Slice selection in MRI uses RF pulses with a narrow bandwidth in combination with a magnetic field gradient to tip over spins within a narrow range of positions. For two RF pulse shapes (A) the resulting slice profiles are shown by plotting the remaining z-magnetization (M_z) after the pulse (B). A simple rectangular RF pulse produces a poor slice profile, but a longer, shaped RF pulse produces a profile closer to a rectangle. With even longer, adiabatic pulses, the profile is even better, as illustrated by the inversion profile (C). With the adiabatic pulse the duration is long enough for relaxation to begin to have an effect. (Adiabatic inversion plot courtesy of L. Frank.)

profile in an imaging experiment. Figure 6.8A shows M_z after an RF pulse with an amplitude and duration matched to give a 90° flip angle on-resonance. Two curves are shown, one for a constant amplitude B_1 throughout the RF pulse and one for a tailored RF pulse in which the amplitude of B_1 is modulated. By modulating the amplitude of B_1 , the frequency selectivity of the pulse, and thus the slice profile, can be improved considerably. The cost of using a shaped pulse, however, is that the duration of the RF pulse is increased. The on-resonance flip angle is proportional to the area under the RF pulse profile, so a constant amplitude pulse is the most compact in time. To create a shaped RF pulse profile with the same

duration and flip angle, the peak amplitude of B_1 would have to be significantly increased, but hardware limitations set the maximum peak amplitude. So it is usually necessary to extend the duration of the RF pulse to produce a cleaner slice profile.

Adiabatic radiofrequency pulses

The slice profile can be further improved by allowing B_1 to vary in frequency as well as amplitude. An *adiabatic RF pulse* is an example that produces a particularly clean slice profile (Frank *et al.* 1997; Silver *et al.* 1985). In an adiabatic pulse, the magnetization is not so much precessing around the effective field as following it as it slowly rotates. To see how this works, imagine starting B_1 far off-resonance. Then B_{eff} is nearly along the z -axis, and the magnetization will precess around it, while remaining nearly parallel to B_{eff} . If we now slowly change the frequency of B_1 , moving it closer to resonance, the effective field will slowly tip toward the x -axis. If this is done slowly enough, so that the magnetization precesses many times around B_{eff} during the process, then M_0 will follow B_{eff} precessing in a tight cone around it, as B_{eff} slowly tips toward the x -axis. As soon as the frequency of B_1 reaches ω_0 , the effective field and M_0 will lie along the x -axis, and the net effect will be a 90° pulse. If the pulse is continued, moving beyond the resonance condition until M_0 is rotated on to the negative z -axis, the net effect is a 180° inversion pulse. As shown in Fig. 6.8C, the slice profile can be quite good. The cost of this, however, is that such RF pulses take a long time to play out because of the need to sweep slowly through frequency. In imaging applications, a standard slice selection pulse may take 3 ms, whereas a good adiabatic pulse may require 20 ms or more.

Finally, an ingenious application of the idea of an adiabatic pulse is the selective inversion of flowing blood using a continuous RF pulse. Calling something a continuous pulse sounds like an oxymoron, but it is actually fairly descriptive: no RF field lasts forever, so really any applied RF field is a pulse, and *continuous* just indicates that it is on for a much longer time (e.g., several seconds) than is typical for a standard excitation pulse. Such pulses are often used in arterial spin labeling (ASL) methods for measuring cerebral blood flow (Alsop and Detre 1996). The goal in such experiments is to invert the magnetization of arterial blood (i.e., flip it 180°) before the blood reaches the tissue of interest and then subtract this tagged image from a control image in which the blood was not inverted. This ASL difference signal is then directly proportional to the amount of blood delivered to the tissue. Continuous inversion works on the same principle as an adiabatic RF pulse, except that B_1 is constant; it is the resonant frequency of the moving spins that is varied. This is accomplished by turning on a gradient in the superior/inferior direction so that as an element of blood moves up the artery toward the head its resonant frequency changes because its position in the gradient field changes. The frequency of the RF pulse is set to correspond to the resonant frequency in a particular transverse plane in the neck or head. When an element of blood is far from this zero plane, B_1 is off-resonance, and so the effective field is nearly along the z -axis. As the blood approaches the zero plane, the z -component of the effective field diminishes as the resonant frequency approaches the RF frequency. When the blood crosses the zero plane, B_{eff} is entirely along x , and as the blood continues, moving off-resonance in the other direction, B_{eff} tips down toward the negative z -axis. If this sweep of B_{eff} is slow enough, the magnetization will follow B_{eff} and end up inverted. This continuous labeling technique produces a steady stream of inverted blood as long as the RF is turned on. Chapter 13 discusses ASL techniques in greater detail.

Magnetic properties of matter

Paramagnetism, diamagnetism, and ferromagnetism

Matter contains several components that possess magnetic dipole moments, and the nuclear spins that give rise to NMR are actually among the weakest. Far more important in determining the magnetic properties of materials are the magnetic dipole moments of unpaired electrons. The dipole moment of an electron is three orders of magnitude larger than that of a proton, and so the alignment of electron magnetic moments in a magnetic field leads to much larger effects. Based on our preceding arguments about the interactions of a magnetic dipole with a magnetic field, we would expect that when a sample is placed in a magnetic field B_0 , the dipole moments in the sample would tend to align with the field, creating a net dipole moment parallel to the field. If the magnetic field is non-uniform, we would expect there to be a net force on the sample drawing it toward the region of higher field.

To test this prediction, that materials should feel a force in a non-uniform field, we could perform an experiment using a standard MR imager. The magnet is typically oriented horizontally, with a uniform magnetic field in the center but a diverging and weakening field near the ends of the bore. Then we would expect that, as a sample of a particular material is brought near to the bore, it would feel a force pulling it into the magnet. Because the magnetization associated with the intrinsic magnetic dipoles is weak, the force on most materials should also be weak, so a sensitive measuring system is required. When this experiment is performed on a variety of materials, some, such as aluminum, are pulled toward the bore with a force on the order of 1% of the weight of the sample, and these materials are described as *paramagnetic*. However, many other materials, such as water, are weakly repulsed by the magnetic field and pushed away from the bore with weaker forces, and these materials are described as *diamagnetic*. Finally, a third class of materials, including iron and magnetite, are strongly attracted toward the magnet, with forces orders of magnitude larger than those of paramagnetic materials. These materials are described as *ferromagnetic*.

From our foregoing arguments about the forces on dipoles in a field, paramagnetism is easily understood and expected. Paramagnetism arises primarily from the effects of unpaired electrons aligning with the magnetic field, with a small additional component from the alignment of nuclear dipoles (Fig. 6.9). But the existence of diamagnetism is unexpected because a repulsive force indicates a net dipole moment aligned opposite to the field. Diamagnetism results from the effects of the magnetic field on the orbital motions of the electrons. An electron orbiting an atom or molecule is effectively a current, and so there is a magnetic dipole moment associated with the orbital state, as well as the spin state, of the electron. The curious feature of these induced orbital dipole moments, however, is that the net dipole moment is oriented opposite to the external magnetic field.

Diamagnetism can be understood in a rough classical physics way by looking at the oversimplified picture of two atoms with electrons orbiting the nucleus in different directions (Fig. 6.9). The orbital magnetic dipole moment is opposite for the two different orbital directions, and both directions of rotation are equally likely. With no magnetic field, the net magnetization is zero. The stability of the electron orbit results from the balance between the inward electrical force and the outward centrifugal force from the electron's velocity. When a magnetic field is added, the additional magnetic force on the electron is inward for one sense of orbital motion and outward for the other. If the velocities of the electrons adjust to

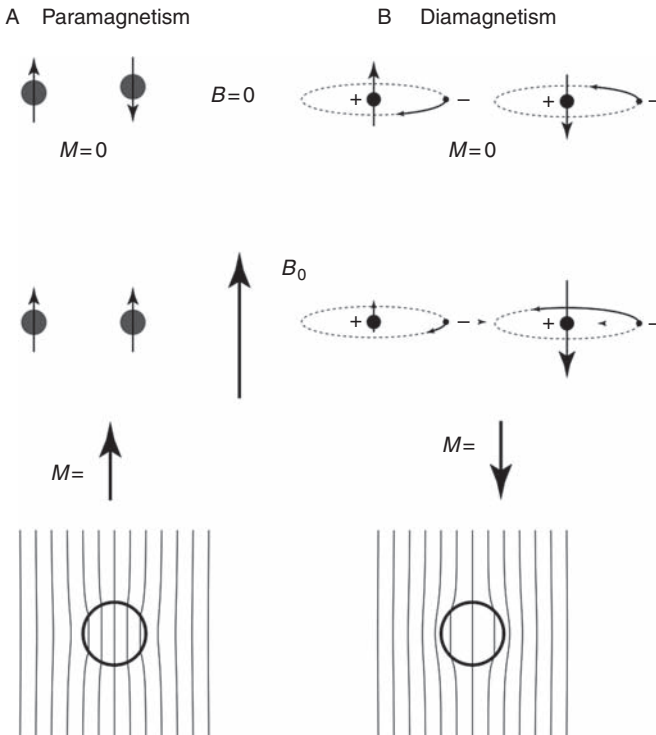


Fig. 6.9. Paramagnetism and diamagnetism. (A) Magnetic dipole moments (unpaired electrons and nuclei) align with the magnetic field to produce a magnetization (M) aligned with the main magnetic field B_0 (paramagnetism). (B) The magnetic dipole moments resulting from the orbital motions of electrons are altered to produce a net magnetization aligned opposite to the field (diamagnetism). For diamagnetism, the diagrams suggest how the added force from the magnetic field either adds to or subtracts from the centrifugal force on the electron; consequently, the electron velocity for stability increases or decreases depending on the direction of motion. The bottom row shows distortions of uniform magnetic field lines by a magnetized sphere.

rebalance the forces, one is sped up and the other slowed down, increasing the magnetic dipole moment aligned opposite to the field and decreasing the other. The net magnetization is then opposite to the field.

All materials have diamagnetic effects as a result of orbital electron motions that create a magnetization aligned opposite to the field, and some materials in addition have paramagnetic effects from the spins of unpaired electrons, which create a magnetization aligned with the field. The net magnetization that results reflects the balance between diamagnetic and paramagnetic effects, and the classification of materials as diamagnetic or paramagnetic reflects the outcome of this balance. But both diamagnetism and paramagnetism are relatively weak effects, in that the magnetic forces on such materials, even in a magnetic field as high as those used for imaging, are still only approximately 1% of the force of gravity.

A striking exception to this discussion of materials that interact weakly with a magnetic field is a ferromagnetic material, which can be strongly magnetized when placed in a magnetic field and can retain that magnetization when the field is removed. The very large magnetization induced in such materials corresponds to the coordinated alignment of many electron spins, although the magnetic interactions of the spins are not responsible for the coordination. In ferromagnetic materials such as iron, unpaired electrons are in a lower

energy state when they are aligned with each other, for reasons related to the quantum nature of the spins. The unpaired electron spins of nearby atoms in a crystal of iron then tend to become aligned with each other, forming a small volume of material with a uniform orientation, called a *domain*. A large block of material consists of many domains, with a random direction of orientation within each domain. Each domain is still microscopic but nevertheless contains billions of atoms, and so the magnetic field associated with the aligned electrons is quite large. In the absence of an external magnetic field, there is no net magnetization because of the random orientation of the domains. When the iron is placed in a magnetic field, the domains aligned with the field are energetically favored, and they begin to grow at the expense of the other domains. That is, the electrons in a neighboring domain switch their orientation to join the favored domains. The result is the creation of a very large magnetization, and even after the external field is turned off the rearranged domain structure tends to persist, leaving a permanent magnetization.

Ferromagnetic materials are always excluded from the vicinity of an MRI system. Small fragments of ferromagnetic material can severely distort MR images. Even a sample as small as a staple can produce a large area of signal dropout in an image. More seriously, the inadvertent use of ferromagnetic tools in the vicinity of a large magnet is a severe safety risk. In the field of a 1.5 T magnet, the magnetic force on a 2 lb (1 kg) iron wrench is more than 50 lb (23 kg), and the wrench will fly toward the scanner. Care should always be taken to check carefully any equipment brought into the MR scan room to ensure that no ferromagnetic components can become dangerous projectiles. In addition, subjects must be carefully screened to ensure that they have no ferromagnetic materials in their body, such as metal plates, old surgical clips, or even small metal fragments from sheet metal work. From here on we will focus only on materials that are weakly magnetized.

Magnetic susceptibility

In addition to the magnetic forces discussed above, a second effect of placing a sample of a material in a magnetic field is that the local magnetic field is distorted by the interaction of the internal dipole moments with the field. Each cubic millimeter of the material contains many magnetic dipole moments, and each of these dipoles creates its own dipole field. In a magnetic field, the dipole moments tend to align with the field if the material is paramagnetic, or opposite to the field if it is diamagnetic, and the sum of the moments of each of these dipoles is the net magnetization of the material. The net magnetization is the equivalent dipole density in the material and so depends on both the intrinsic dipole density and the degree of alignment of the dipoles.

The creation of a net magnetization has two important effects for MR imaging. The first is that the part associated with the alignment of nuclear dipoles is the magnetization that can be manipulated to generate the NMR signal. The second effect is that other dipole moments, such as unpaired electrons, contribute a much larger net magnetization, and this creates an additional, non-uniform magnetic field that adds to the main field B_0 . For example, the effect on the total magnetic field of placing a sphere of diamagnetic or paramagnetic material in a uniform field is illustrated in the bottom row of Fig. 6.9. In the absence of the sphere, the field lines are vertical and parallel. For a paramagnetic sphere, the field lines are pulled in and concentrated within the sphere, and for the diamagnetic sphere the lines are pushed out from the sphere. These field inhomogeneities produce distortions and signal loss in MR images, but they also are the basis for functional imaging exploiting the BOLD effect or using injected contrast agents.

The degree to which a material becomes magnetized is measured by the *magnetic susceptibility*, χ , of the material: the local magnetization M is χB_0 . As M has the same dimensions as B_0 ,

χ is dimensionless. This can be a bit confusing because M is the equivalent density of magnetic dipoles, rather than a magnetic field, despite the fact that they have the same units. The magnetic fields produced in the neighborhood of a magnetized body are of the same order as M , but they also depend on the geometrical shape of the body. For most materials, the value of χ is of the order of a few parts per million, so the additional weak field that results from the alignment of intrinsic magnetic dipoles in matter is typically only a few parts per million of B_0 . The susceptibility χ may be positive (paramagnetic) or negative (diamagnetic), depending on whether the component of magnetization resulting from the unpaired electrons or the component from the orbital motions is dominant. Exogenous contrast agents used in MRI are paramagnetic.

It is important to maintain a clear distinction between the local magnetization of a magnetized body and the magnetic field created by that magnetized body. Whenever a body with a uniform composition is placed in a uniform magnetic field, it becomes uniformly magnetized. This means that in any small volume of the body, the partial alignment of the magnetic dipoles of the body is the same, so they add up to a uniform magnetization throughout. All this is independent of the shape of the body; it is a direct effect of the interaction of each of the dipoles with the magnetic field, leading to partial alignment. A collection of partially aligned dipoles, in turn, creates its own magnetic field through all of space, and this field adds to B_0 . This additional field depends strongly on the geometry of the body.

However, if the local magnetization of a body depends on the partial alignment of the dipoles with the local field, and the local field is then altered by the additional field produced by the magnetized body, would this feed back on the local magnetization itself and alter it? The presence of the magnetized body does alter the local field, and indeed this does alter the local magnetization, but by a negligibly small amount. The field distortions in the human head are only approximately 1 ppm of B_0 , so the variations in the local magnetization from this additional field are only 1 ppm of 1 ppm, and so are negligibly small. For practical purposes then, we can assume that a body of arbitrary shape but uniform composition, when placed in a uniform magnetic field B_0 , becomes uniformly magnetized with a dipole moment density $M = \chi B_0$.

The field distortions around a magnetized body depend on the shape of the body. Figure 6.10 shows the pattern of field offsets around a uniformly magnetized sphere. For this simple spherical geometry, field distortion is again a dipole field pattern. That is, adding up the contributions from each of the individual dipoles produces a field that is equivalent to one big dipole at the center of the sphere. However, this is only true for the perfect symmetry of a sphere; a body with a more complex shape would produce a more complex field distortion. Another simple geometrical shape that is relevant for fMRI is a long cylinder oriented perpendicular to the magnetic field (Fig. 6.10). The field distortion is qualitatively similar to the distortion around a sphere, although the radial dependence is different: the field offset falls off as $1/r^3$ for the sphere, but $1/r^2$ for the cylinder (r is the radial distance). At the surface of the cylinder, the maximum field offset ΔB is $2\pi\Delta\chi B_0$, where $\Delta\chi$ is the susceptibility difference between the inside and the outside of the cylinder, and this maximum offset is independent of the radius of the cylinder. A magnetized cylinder is a useful model for thinking about blood vessels magnetized by the presence of deoxyhemoglobin and the resulting BOLD effect.

In the preceding discussion we have focused on the field distortions outside a magnetized body, but for most shapes the field inside is distorted as well. The sphere and the infinitely long cylinder are special cases in that they produce a uniform field offset inside. A short cylinder produces an external field intermediate between that of a sphere and a long cylinder, and the internal field is also distorted.

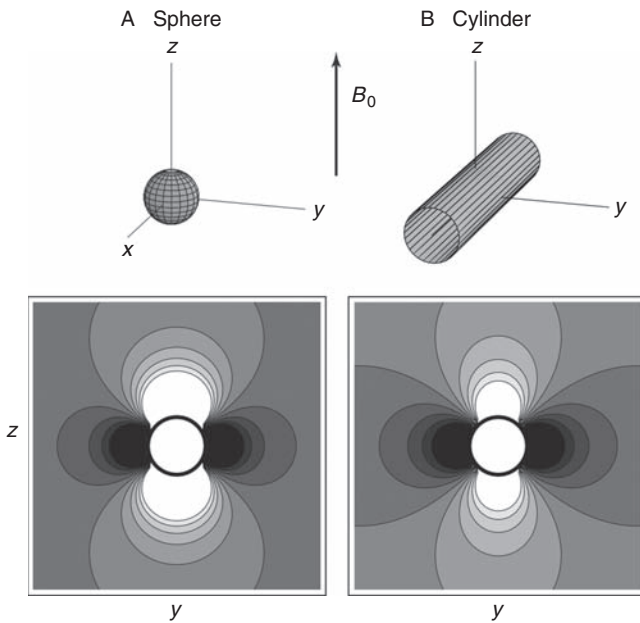


Fig. 6.10. Magnetic field distortions around magnetized objects. Contour plots of the offset of the z -component of the field, B_z , in a plane cutting through a uniformly magnetized sphere (A) and cylinder (B). Both patterns have a dipole-like shape.

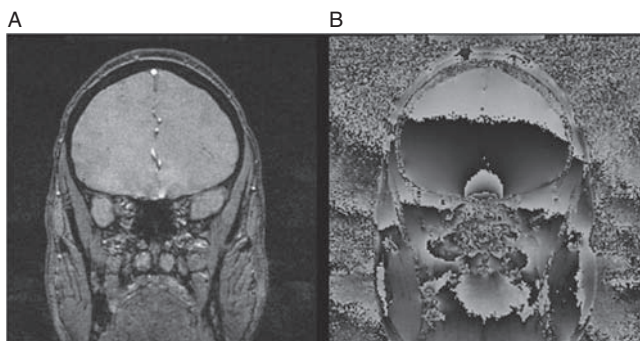


Fig. 6.11. Magnetic field distortions in the head. A coronal gradient echo image, showing magnitude (A) and phase (B). The phase map shows magnetic field distortions owing to the heterogeneity of the brain. Distortions include a dipole-like field near the sinus cavity and a superior–inferior gradient.

Field distortions in the head

The significance of these magnetic susceptibility effects is that whenever a body is placed in a uniform, external magnetic field B_0 , the net field is distorted both outside and inside the body. This happens even if the body has a perfectly uniform composition and depends strongly on the shape of the body. Furthermore, if the body is heterogeneous, composed of materials with different magnetic susceptibilities, the field distortion is even worse. Figure 6.11 (shown also as Fig. 4.10) shows the field distortion within a human head when it is placed in a uniform magnetic field. To a first approximation, the head consists of three types of material: water, bone, and air. Field distortions are evident in the vicinity of interfaces between these materials. The large sinus cavities produce a local field distortion rather like a dipole field, which extends through several centimeters of the brain, and also there is a broad field gradient in the superior–inferior direction caused by the presence

of the rest of the body. In general, the size of the field distortion in terms of the volume affected is comparable to the size of the heterogeneity. The largest field offsets result from the air–water interface near the sinus cavities. Detailed modeling of the air spaces of the head predict field offsets of a few parts per million, in good agreement with what is measured (Li *et al.* 1995).

In MRI such field distortions within the body are a nuisance. A central assumption of MRI is that the magnetic field is uniform so that any field offsets measured when the field gradients are applied are entirely a result of the location of the source of the signal, and not caused by intrinsic field non-uniformity. Field distortions caused by magnetic susceptibility variations between tissues thus lead to distortions in the MR images, and for some imaging techniques (e.g., EPI) these distortions can be severe. For this reason, MR scanners are equipped with additional coils called *shim coils*, which can be used to flatten the magnetic field. This process is called *shimming* the magnetic field, and it is important to remember that this involves correcting for the intrinsic inhomogeneities of the human body as well as for non-uniformities of the magnet itself.

The macroscopic field distortions shown in Fig. 6.11 are an unwanted byproduct of tissue heterogeneity. However, *microscopic* field distortions around small blood vessels are the basis for both contrast agent studies of blood volume and BOLD-fMRI. A gadolinium-based contrast agent alters the susceptibility of the blood, creating field offsets in the space around the vessels (Villringer *et al.* 1988). At the peak of the passage of a bolus of Gd-DTPA through the vasculature, the susceptibility change of the blood is approximately 0.1 ppm (Boxerman *et al.* 1995), and if we model the vessels as long cylinders, this produces maximum field offsets of approximately 0.6 ppm. The BOLD effect is based on the fact that during brain activation the O₂ content of the venous blood is increased, which in turn alters the blood susceptibility relative to the surrounding tissue water. The susceptibility change owing to increased oxygenation of the blood in the activated state is on the order of 0.01 ppm (Weisskoff and Kiihne 1992), so the maximum field offsets are approximately 0.06 ppm. Because the susceptibility difference between the blood and the surrounding water is reduced when the blood is more oxygenated, the signal increases slightly. Magnetic susceptibility effects relevant to fMRI thus span nearly two orders of magnitude, from the large-scale heterogeneity of the brain that produces field variations of a few parts per million and image artifacts, to BOLD microscopic susceptibility differences of a few hundredths of a part per million, which reveal areas of functional activity.

References

- Alsop DC, Detre JA (1996) Reduced transit-time sensitivity in non-invasive magnetic resonance imaging of human cerebral blood flow. *J Cereb Blood Flow Metab* **16**: 1236–1249
- Boxerman JL, Hamberg LM, Rosen BR, Weisskoff RM (1995) MR contrast due to intravascular magnetic susceptibility perturbations. *Magn Reson Med* **34**: 555–566
- Feynman RP, Leighton RB, Sands M (1965) *The Feynman Lectures on Physics*. New York: Addison-Wesley
- Frank LR, Wong EC, Buxton RB (1997) Slice profile effects in adiabatic inversion: application to multislice perfusion imaging. *Magn Reson Med* **38**: 558–564
- Grant PE, Vigneron DB, Barkovich AJ (1998) High resolution imaging of the brain. *MRI Clin N Am* **6**: 139–154

- Li S, Williams GD, Frisk TA, Arnold BW, Smith MB (1995) A computer simulation of the static magnetic field distribution in the human head. *Magn Reson Med* **34**: 268–275
- Purcell EM (1965) *Electricity and Magnetism*. New York: McGraw-Hill
- Silver MS, Joseph RI, Hoult DI (1985) Selective spin inversion in nuclear magnetic resonance and coherent optics through an exact solution of the Bloch–Riccati equation. *Phys Rev A* **31**: 2753–2755
- Villringer A, Rosen BR, Belliveau JW, *et al.* (1988) Dynamic imaging with lanthanide chelates in normal brain: contrast due to magnetic susceptibility effects. *Magn Reson Med* **6**: 164–174
- Weisskoff RM, Kiihne S (1992) MRI susceptometry: image-based measurement of absolute susceptibility of MR contrast agents and human blood. *Magn Reson Med* **24**: 375–383